Tunable Silicon Photonic Circuits for Telecommunications Applications / (TSPC)

2021

Call for Proposals 2021 - AASTMT

Electronics and communications Engineering, Cairo-Heliopolis

Table of Contents

Keywords: Silicon on silica, silicon photonics, optical communications, integrated circuits, electro-optic modulators, tunable optical circuits, Mid-infrared silicon modulators.

Funding and Duration: 12 Months for the CRP

Total cost: 280,000 LE

Research Theme: Electronics and Communication Engineering

1. Proposal Summary

In this project, an integrated optical modulator is investigated. The proposed modulator circuit is based on the silicon-on-silicon platform. This platform proved very promising since it is the standard in the well-established electronic devices industry. Therefore, the proposed device capitalizes on the already available industrial infrastructure that has been very rewarding for decades. However, introducing photonics, alongside electronics, on this platform enables much higher speeds of operation. This approach eventually aims at overcoming the minimum-feature-size bottle-neck that is hindering the advancement of electronic circuits.

The electro-optical modulator exploits different modulation techniques such as plasma dispersion effect and electro-optic materials. In the plasma dispersion, doped silicon material is exposed to the modulating signal which changes the charge concentration and hence the refractive index of silicon. This leads to a phase modulation of the laser power passing through. Electro-optical materials, such as polymers, on the other hand, can introduce a phase shift without doping.

The proposed modulators represent a crucial element in optical communications. Such devices convert electrical data to optical and hence enable communications over optical fibers and free-space laser links. In modern days, optical fibers contribute a big part to the ultra-high-speed internet links which in turn are necessary for cutting-edge applications such as the internet of things (IoT).

Exploring such possibilities is not new to our team which possesses a vast experience in this field with proven successes, theoretically and experimentally, as detailed in the researchers' information section. However, in this new work, we intend to utilize our previously published results in designing new types of circuits and also extend our work to cover lightly explored areas such as the mid-infrared range. In the mid-infrared region, more advantages in the design can be realized, such as less sensitivity to fabrication tolerance and stronger modulation effects.

Our team aims at using simulation tools, that proved very effective, from Lumerical [1]. We have a deep knowledge of such tools as DEVICE, MODE and FDTD which we used for our recently published work. Also, we will be studying potential optical material candidates using spectrometers.

في هذا المشروع ، يتم فحص مُعدِّل بصري متكامل. تعتمد دائرة المعدل المقترحة على منصة السيليكون على السيليكا. أثبتت هذه المنصة أنها واعدة للغاية لأنها المعيار في صناعة الأجهزة الإلكترونية الراسخة. لذلك ، يستفيد الجهاز المقترح من البنية التحتية الصناعية المتاحة بالفعل والتي كانت مجزية للغاية لعقود. ومع ذلك ، فإن إدخال الضوئيات ، إلى جانب الإلكترونيات على هذه المنصة يتيح سرعات تشغيل أعلى بكثير. يهدف هذا النهج في النهاية إلى التغلب على عنق الزجاجة ذي الحد الأدنى من حجم الميزة والذي يعيق تقدم الدوائر الإلكترونية.

يستغل المغير الكهروضوئي تقنيات التعديل المختلفة مثل تأثير تشتت البلازما والمواد الكهروضوئية. في تشتت البلازما ، تتعرض مادة السيليكون المخدر لإشارة التعديل التي تغير تركيز الشحنة وبالتالي معامل الانكسار للسيليكون. هذا يؤدي إلى تعديل طور لقوة الليزر التي تمر عبرها. من ناحية أخرى ، يمكن للمواد الكهروضوئية ، مثل البوليمرات ، أن تحدث تحولاً في الطور دون تعاطي المنشطات.

تمثل المغيرات المقترحة عنصرًا حاسمًا في الاتصالات الضوئية. تقوم هذه الأجهزة بتحويل البيانات الكهربائية إلى بصرية ، وبالتالي تتيح الاتصالات عبر الألياف الضوئية وروابط الليزر في الفضاء الحر. في العصر الحديث ، تساهم الألياف الضوئية بجزء كبير في روابط الإنترنت فائقة السرعة والتي تعد بدورها ضرورية للتطبيقات المتطورة مثل إنترنت الأشياء(IoT).

استكشاف مثل هذه الاحتمالات ليس جديدًا على فريقنا الذي يمتلك خبرة واسعة في هذا المجال مع نجاحات مثبتة، من الناحية النظرية والتجريبية، كما هو مفصل في قسم معلومات الباحثين. ومع ذلك ، في هذا العمل الجديد ، نعتزم الاستفادة من نتائجنا المنشورة سابقًا في تصميم أنواع جديدة من الدوائر وكذلك توسيع نطاق عملنا ليشمل المناطق التي تم استكشافها قليلاً مثل نطاق الأشعة تحت الحمراء المتوسطة. في منطقة الأشعة تحت الحمراء المتوسطة ، يمكن تحقيق المزيد من المزايا في التصميم ، مثل حساسية أقل لتحمل التصنيع وتأثيرات تعديل أقوى.

و يهدف فريقنا إلى استخدام أدوات المحاكاة التي أثبتت فعاليتها الكبيرة من Lumerical و التي لدينا معرفة عميقة بأدواتها مثل DEVICE و MODE و FDTD التي استخدمناها في أعمالنا المنشورة مؤخرًا .أيضا ، سوف ندرس مواد بصرية محتملة باستخدام أجهزة قياس الطيف.

2. Introduction

The new era of internet of things (IoT) and the fifth generation (5G) of telecommunications mobile systems place demands of ultra-high-speed modulation [2]. With such new technology, many devices of the daily-life applications are required to be connected to the wired and wireless networks. This requires a huge bandwidth for the backbone circuits of such networks. As stated in [2], the state-of-the-art communications speed requirements are: $1\ Pbps$ for the core transport, $1\ Tbps$ for the metro transport, $100\ Gbps$ for the backhaul truck and finally $1-10\ Gbps$ for the end user devices.

For decades, silicon microelectronics industry has developed rapidly improving performance, functionality, and integration density of integrated circuits. In parallel to this downscaling of components, tens of millions of wafers per year at the 300-mm wafer scale were produced. This outstanding level of commercial development has yielded low cost, high performance electronic devices.

To be in line with the demand for the huge amount of data transfer, the need for high bandwidth interconnects is raised to enhance computing capability [3]-[4]. Interconnects are fabricated from copper in traditional electronic ICs. As the integration density increases, the physical limitation of the electrical interconnects starts to emerge. Current electrical interconnects experience a high crosstalk effect when the data rate is increased. The crosstalk is the undesired effect of the transmitted signal between the network parts. Therefore, this well-known interconnect bottleneck formed a serious challenge to this striving industry.

On the other hand, photonic devices stayed bulky, expensive, and modular in nature, with inequality in progress in high-density integration in silicon-based electronics. To address this discrepancy and to provide a solution to the interconnect bottleneck problem, the transfer from traditional electronics to optical data transmission has been unavoidable. This fact paved the way to propose silicon photonics (SiP) where complementary metal-oxide-semiconductor (CMOS) fabrication process and materials could be used to make photonic components with high-integration densities. The idea is that you can take all of the technologies that have been developed for electronics – for example, the ability to fabricate devices at the nanoscale - and use that technology to produce waveguides and other components that enable the transmission of light through the chip in the same way a wire would transfer electric current [5]. This way, advantageous optical interconnects, which support low-dispersion communications and low cross-talk within high bandwidth can be integrated using CMOS technology [3].

Therefore, over the last three decades, a lot of research was invested in photonic integrated circuits (PICs). The integration of electro-optic devices with small footprint on a chip can allow for more scalable and lower power consuming devices [4]. Through decades of research, many photonic devices have reached maturity such as fiber grating-couplers [6], [7] which are used to couple a laser beam from an external source to a silicon chip, sensors [8], logic circuits [9], polarization rotators [10] , integrated gyroscopes [11], channel interleavers [12], and most importantly, electro-optic modulators [13]–[17] which are devices that load the electronic data to a laser carrier. With such a platform, the traditional bottleneck of electrical interconnection delay can be overcome [18] employing the ultimate speed in universe, the speed of light.

The CMOS platform is an ideal design space for PICs due to the high refractive index contrast achieved between Si, Ge, SiO_2, Si_3N_4, and other dielectrics. Using any combination of these materials along with silicon-on-insulator (SOI) platforms provide a platform for high-speed and low-dispersion applications, maintaining the mature CMOS technology.

Silicon photonics (SiP) became a leading technology for optical modulators at relatively wide wavelengths from $1.3\ \mu m$ to $1.63\ \mu m$. This technology can achieve functions that are already done by using expensive materials based on III-V semiconductor [19], [20]. Silicon is more attractive than III-V materials for many reasons. One reason is that silicon has a relatively high refractive index at the near infrared (NIR) and mid infrared (MIR) wavelengths, which enables miniature structure and high fabrication density. But what gives SiP an upper hand – regardless of the limits of using of silicon as a photonic material– is its compatibility with CMOS technology which provides a low-cost platform, especially for mass production. This also allows the integration of passive and active photonic devices as well as the integration of photonics with electronics in a single chip [4].

For the aforementioned reasons, our team took interest in developing electro-optic modulators using the silicon-on-silica platform which is CMOS compatible. Recently, we have produced many publications [13]–[17] in this direction. The modulators we proposed are based on the plasma dispersion effect where doped silicon waveguides are tuned using a modulating voltage applied to nearby electrodes. The proposed designs show competitive performance as detailed in our papers.

We will also keep relying on the simulation package from Lumerical [1] which proved successful in our previous phase of the work. With this package, the electronics part of the modulator is simulated using DEVICE. The results from DEVICE, which give the charge density distribution versus voltage, can then be exported to MODE where optical simulations are performed to show the optical power modulation.

3. Project Objectives

a) In this work, we are planning on integrating silicon-on-silica platform into more complex photonic circuits such as ring resonators (RRs), multimode interferometers (MMIs), beams steerers and polarization converters (PCs). The expected outcome is high-speed circuits that serve in data routing and modulation.

b) We are also planning on extending the range of the carrier wavelength to the mid-infrared range ($\sim 3\ \mu m$) which attracted a lot of attention recently [21]. In this range, modulators are more fabrication tolerant because of the inherent size of the device, less scattering loss effects and stronger plasma-dispersion effect. One more attraction in this range is the ability of sensing gases which have their absorption fingerprint in this range of wavelength [22]. This means that having electro-optic modulators in this range will make them integrable in a bigger system that includes other functionalities such as sensing.

c) In our plan, we will also be investigating new optical materials. These materials are basically doped polymers which can stick to silicon-based chips and might be utilized in the tuning of electro-optic modulators. In this regard, we will rely on our experience [23]–[26] in charactering polymers using spin coater, spray coater, and optical spectrometers. This is also a booming direction of research with lots of potential.

4. Project Description

4.1 A general background

In our recent publications [13]–[17], we introduced new designs of electro-optic modulators using the integrated silicon-on-silica (SOI) technology. The designs relied on the plasma dispersion in doped-silicon waveguides. In this project we intend to build on this recent success and introduce tunable structures based on our modulators as detailed next.

In this line of work, the mature silicon-on-silica technology is adopted. The direct reason for this choice is that this is the standard platform for the mature electronic circuits industry. The availability of the fabrication facilities around the globe at low cost is a big edge over other platforms than can serve in the photonic circuits domain. Therefore, silicon photonics has attracted so much investment and witnessed tremendous growth over the past two decades [27], [28].

The basic element in photonics is the optical waveguide. The waveguide is the path that guides light to propagate from one point to another. A waveguide of small size and low loss is usually highly desirable. In this technology a waveguide is formed using silicon core, surrounded by smaller refractive index materials. The refractive index of silicon, n_{si} , is approximately 3.5 at typical telecommunications wavelengths of $1.3\ \mu m$ and $1.55\ \mu m$. In this technology, silicon is placed on top of a buried silicon dioxide layer, also known as silica, the refractive index of which, n_{silica}, is typically 1.5. The cladding surrounding silicon could be just air, of refractive index $n_o = 1$, or other materials such as silica or polymers. With this contrast of refractive index between the silicon core and the surrounding materials, optical power can be guided inside silicon. Besides, the big contrast in the refractive index adds more features to the waveguide action. This includes the capability of manufacturing waveguides of relatively smaller cross-sectional area. Also, with a big refractive index contrast, the waveguide bending can be achieved with a very small radius, down to $3\ \mu m$, with relatively low optical losses. This simply means higher fabrication density, i.e., packing more devices in smaller chip area which reduces the fabrication cost. This waveguide is the building unit of more complex photonic circuits such as Mach-Zehnder interferometers (MZIs), ring resonators (RRs), multimode interferometers (MMIs), polarization converters (PCs), beam steerers and arrayed waveguides [29].

However, applications that rely on modulation require materials with a tunable refractive index. The desired tuning mechanism is usually changing the refractive index under an externally applied electric field. The ability of the material to provide such response is given by its electro-optic coefficient. Therefore, materials that possess high electro-optic coefficients, such as $LiNbO_3$, found immediate use in industry [30], [31]. Unfortunately, despite the strong advantages of the silicon-on-silica technology, the electro-optical coefficient of silicon is relatively small and therefore silicon shows unacceptably small response to the modulating electric field. It is also useful to mention that silicon possesses a high thermo-optic coefficient, meaning its refractive index is much more sensitive to temperature. This allowed researchers to utilize silicon in thermal modulator applications. In this type, the modulating data stream in the form of electric current flowing throw metallic wires that are integrated nearby the waveguide. The current heating effect can then alter the waveguide refractive index and induce phase changes to the propagating light. However, this technique cannot provide modulation speeds above the range of a few MHz [32] which has become way slower than the requirements of modern applications.

This issue was overcome by the revolutionary study by Soref and others [33]. In this solution, doping silicon provides free carriers, electrons and holes, which alter the silicon refractive index according to the following two equations for the wavelength of $1.5\ \mu m$.

$$\Delta n = \Delta n_e + \Delta n_h = -\ [8.8\ x\ 10^{-22} *\ \Delta N + 8.5\ x\ 10^{-18} *\ (\Delta P)^{0.8}]$$
$$\Delta \alpha = \Delta \alpha_e + \Delta \alpha_h = 8.5\ x\ 10^{-18} *\ \Delta N + 6.0\ x\ 10^{-18} *\ \Delta P]$$

Where:
Δn_e is the refractive index change due to electron concentration change
Δn_h is the refractive index change due to hole concentration change
ΔN is the electron concentration change in cm^{-3}
ΔP is the hole concentration change in cm^{-3}
$\Delta \alpha_e$ (in cm^{-1}) is the absorption coefficient changes due to ΔN
$\Delta \alpha_h$ (in cm^{-1}) is the absorption coefficient variation due to ΔP

Now, an externally applied voltage, can change the carrier concentration across the waveguide. This means that the modulating data, in the form of the applied voltage, can alter the refractive index of silicon and hence induce phase changes to the propagating light beam. Therefore, this technique relies on plasma dispersion for modulation and, hence, shows speeds in the range of tens or even hundreds of GHz . This is why this field of research attracted lots of attention since the beginning.

In our recent publications, we proposed electro-optic modulators based on MZIs, like the one show in Fig. 1. In this structure, the two arms of the MZI are p-doped and are surrounded by metallic electrodes. The electrodes are connected to the modulating voltage. The laser beam propagates through the input waveguide toward the first Y-junction where it splits into two beams propagating in the two arms. In each arm, the beam interacts with a tunable refractive index through plasma dispersion. The two beams then interfere at the second Y-junction before laser exists the device from the output side. The interference can then uncover the phase difference between the two arms which reflects on the output light power. Now that the arms are designed identical in length, the propagating modes are in phase if the applied modulating voltage, v , is zero. In other words, the modes interfere constructively. This can be called the ON state. Then, with different voltages applied to the MZI arms, known as the push-pull technique, dispersion effects show, and the two light modes experience different phases and hence the output power is low. This is the OFF state where the modes interfere destructively. Ideally, the phase difference is π for a perfect destructive interference.

In the push-pull technique, one of the two arms shows charge accumulation and the other charge depletion. This way, the required voltage for modulation is distributed over the two arms which means less voltage applied per arm and consequently the applied electric field can be well below the breakdown limit of the used materials.

The parameters used to describe the performance of the modulator include the speed of operation, also called the bandwidth (BW), the modulation voltage (v), the extinction ratio (ER), and the insertion loss (IL). Clearly, it is desired to maximize the bandwidth and minimize the modulation voltage. As for the extinction ratio, it is defined as the ratio of the ON state output power to the OFF-state output power. This parameter should be maximized to reduce the effect of noise on the received signal. The insertion loss is the total optical power loss, i.e., the difference between the input and output power, in the ON state. This parameter should be minimized. The modulators we proposed showed very competitive numbers as detailed in our publications [13]–[17], and therefore, it is time to build on this achievement and take these designs to the next level.

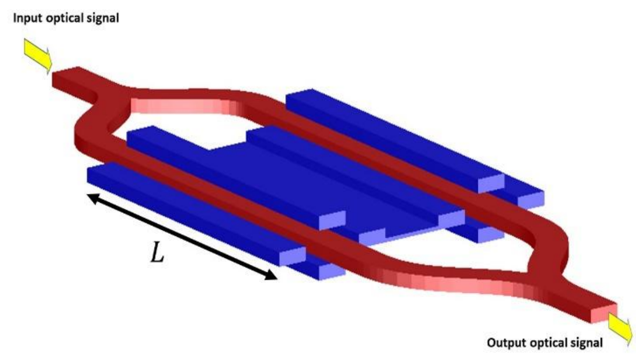

(a)

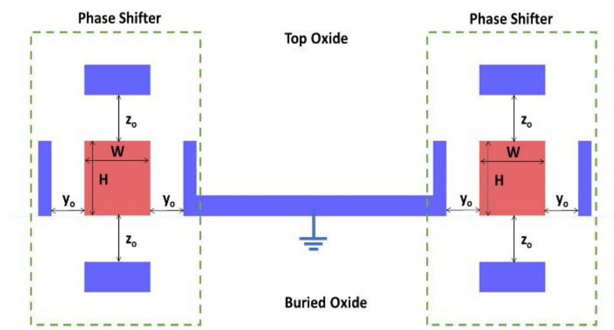

(b)

Fig.1: A Gate-All-Around push-pull modulator with the metallic electrodes in blue, the silicon core in red and the oxide in white (a) a 3D Schematic (b) a cross section of the modulator. The cross section is taken in a plane normally to the signal propagation direction and in the in the middle of the MZI modulator [16].

4.2 The project targets

The project targets can be put in three categories:

Category 1: Using the silicon-on-silica platform to enhance the modulator performance or introduce different functionality. In this category, possible devices to design are:

A) Ring resonators (RRs):
With RRs [34], we expect an enhancement of the general performance of the modulation. The reason for that is the feedback mechanism provided by RRs. This means higher selectivity, i.e., higher quality factor. Besides, RRs usually save fabrication area and enable high fabrication density. The challenge here is look after the bending losses and the free spectral range (FSR) restrictions.

B) Multimode interferometers (MMIs):

The MMI [35], [36] has the advantage of being more fabrication tolerant. The structure is required to be large enough to accommodate multimode fields and therefore is less sensitive to fabrication errors. Besides, the optical power in this device is less prone to scattering losses, again because of the relatively big size. This device found a lot of interest in beam splitting because of its straight-forward design rules. With the tuning mechanism of ours, the MMI can be used as a tunable beam splitter at high speeds.

C) Polarization converters (PCs):
A PC is a device that flips the polarization state of the propagating mode between transverse electric (TE)-like and transverse magnetic (TM)-like [37]. With our tuning technique, this device can be used as a high-speed polarization modulator which is one of the most common modulator types in this field of research. The challenge here is controlling the ratio of power between the two states of operation and the modulation losses.

D) Beam steering:
The beam steerers [38] found recent interest in integrated optics because they provide the means of controlling laser beam direction in free space. In this technique, the phase of the beam is manipulated such that the direction of wavefront is controlled. Our tuning mechanism can therefore be integrated to this this device to provide the phase control at high speeds.

Category 2: In this category we intend to explore modulation in the mid-infrared range (wavelength $\sim 3\ \mu m$). The anticipated advantages include stronger plasma dispersion effect and hence better modulation, less scattering losses besides using large devices that are less sensitive to fabrication tolerance. While the same modulation idea can be applied, there will be challenges regarding the device dimensions and losses.

The dimensions of the waveguides will be larger to accommodate modes at higher wavelengths. This means a challenge on the positioning of the metallic electrodes and the required modulating voltage. Also, leakage losses can increase unless the buried layer becomes larger in thickness. We believe that a careful step-by-step design approach that comprehensively tackles these issues will lead to competitive solutions to these challenges, while keeping the advantage of high-speed of operation.

In our recent publications, we relied on the simulation tools provided by Lumerical [1]. These tools include DEVICE for the electronics part and MODE for the photonics part of the simulations. The results of the electronic change distribution are first acquired from DEVICE before they are exported to MODE to see the effect on the optical mode. The simulator is widely used in this field [39] and have the intention to continue using it.

Category 3: In this category of work, we will explore new optical materials which can play a role in the fabrication of integrated optical circuits in the future. In previous works [25], [26], we employed tunable polymers in designs of electro-optic polymers. More recently, we took interest in the fabrication and characterization of doped polymers [23], [24]. In this work, polymers are fabricated, and their refractive indices are measured versus wavelength for different doping doses. The aim of this line of work is to fabricate materials with characteristics that fit optical circuit design such as low propagation losses at the telecommunications wavelengths and possibly tunable refractive index with strong electro-optic coefficients.

In general, with the cumulative experience of our team members and the ready ideas from our recent work, the project can be a successful continuation of our efforts in this field with many publications expected to be produced.

5. Research Design and Methods

We intend to carry on with numerical simulations from Lumerical [1], which we used successfully in our recent publications [13]–[17]. In short, in this approach, the electric part of the electro-optic modulator is simulated using DEVICE, which is one of two components of the simulator. The charge distribution obtained from DEVICE is then exported to the other component, MODE, which is responsible for the simulation of the optical part of the modulator. Such simulators are usually referred to as Technology Computer Aided Design (TCAD) [40]. The details of the physics behind these numerical solvers are given in the next sections.

5.1 DEVICE: Charge Transport Solver Physics

This simulator calculates the free carrier density as a function of applied voltage. The tool self-consistently solves Poisson's equation [1] that describes the electrostatic potential and the drift-diffusion equation. Hence, the spatial dependence of the free charges (electrons and holes) can be found. Different physical models are included such as carrier recombination (Shockley–Read–Hall, Auger, stimulated and spontaneous emission), carrier transport across hetero-junctions (e.g., between silicon and germanium), electronic band structures, defects, traps, interface states, mobility, temperature dependence, etc. In addition, the fabrication process parameters can be considered to obtain realistic doping and stress profiles. The Charge Transport (CHARGE) solver is a physics-based electrical simulation tool for semiconductor devices, which self-consistently solves the system of equations describing the electrostatic potential and density of free carriers. The drift-diffusion model produces accurate results for a wide range of semiconductor devices in normal conditions. CHARGE solves the drift-diffusion equations for electrons and holes [41],

$$J_n = q\mu_n nE + qD_n\nabla_n$$
$$J_p = q\mu_p pE + qD_p\nabla_p$$

where $J_{n,p}$ is the current density (A/cm^2), q is the positive electron charge, $\mu_{n,p}$ is the mobility, E is the electric field, $D_{n,p}$ is the diffusivity, and n and p are the densities of the electrons and holes, respectively. The mobility $\mu_{n,p}$ of the electrons and holes describes the ease with which carriers can move through the semiconductor material, and is related to the diffusivity $D_{n,p}$ through the Einstein relation [41],

$$D_{n,p} = \mu_{n,p}\frac{K_b T}{q}$$

where K_b is the Boltzmann constant. The mobility is a key property of the material, and may be modeled as a function of temperature, impurity (doping) concentration, carrier concentration, and electric field. In order to determine the electric field, Poisson's equation is solved [41]:

$$-\nabla \cdot (\varepsilon\nabla V) = q\rho$$

where ε is the dielectric permittivity, V the electrostatic potential ($E = -\nabla V$) and ρ the net charge density,

$$\boldsymbol{\rho = p - n + C}$$

which includes the contribution C from the ionized impurity density.

Finally, the auxiliary continuity equations are required to account for charge conservation [41]

$$\frac{\partial n}{\partial t} = \frac{1}{q}\nabla \cdot J_n - R_n$$
$$\frac{\partial p}{\partial t} = -\frac{1}{q}\nabla \cdot J_p - R_p$$

where $R_{n,p}$ is the net recombination rate - the difference between the recombination rate and generation rate. The physical processes associated with the material are assumed to act equivalently when applied to electrons or holes, and as a result, $R = R_n = R_p$.

CHARGE uses an unstructured, finite-element mesh, as shown in Fig. 2. The basic simulation quantities such as material properties, geometry information, electrostatic potential, and carrier concentrations are calculated at each mesh vertex. A finer mesh will better approximate the exact solution to the system of equations, but at resources cost. CHARGE provides a number of mesh mechanisms, including the automatic and guided mesh refinement, that allow the user to obtain accurate results, while minimizing computational effort.

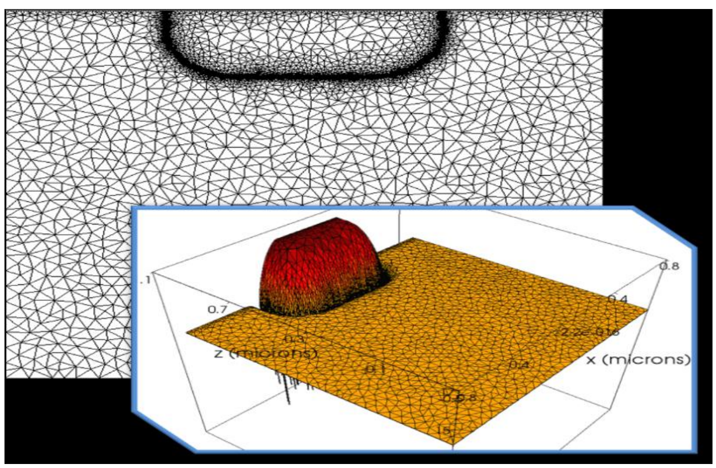

Fig. 2: CHARGE solver mesh structure [1]

Typical results of the distributions of electrons and holes under an applied electric field are shown in Fig. 3.

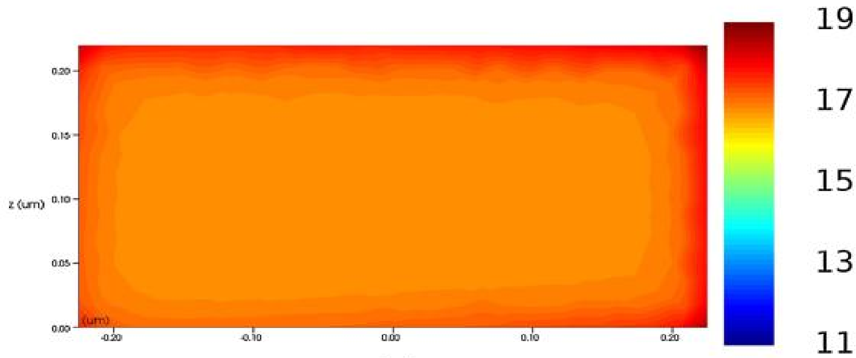

(a)

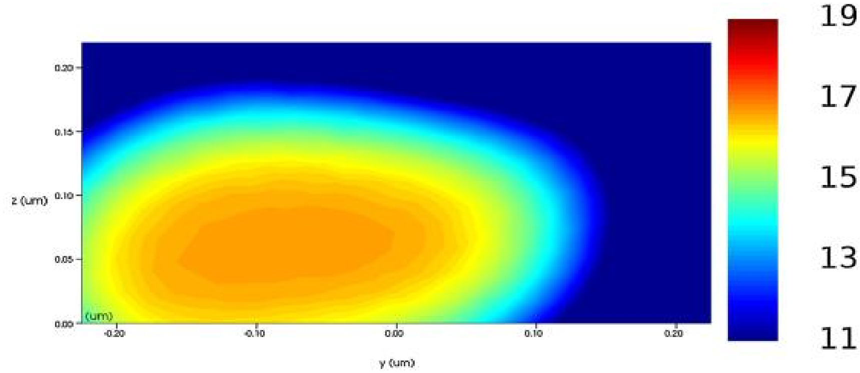

(b)

Fig. 3: A logarithmic scale colormap of the concentration of holes in cm^{-3} over a silicon waveguide cross section in the (a) accumulation mode and (b) depletion mode. [15]

5.2 MODE: Optical waveguide mode solver

This is a Finite Difference Eigenmode (FDE) solver of Lumerical MODE simulation to solve Maxwell's equations on a cross-section of arbitrary wave guide at a specific frequency. The solver calculates the mode field profiles, effective index, and optical propagation losses. A waveguide mode is a transverse field distribution that propagates along the waveguide without changing shape, i.e. the solution is time-invariant [40]. An example mode profile is shown in Fig. 4. If the propagation direction is along the z-axis, then for a z-normal eigenmode solver simulation example shown in Fig. 5, the vector fields are:

$$E(x,y)e^{i(-\omega t+\beta z)}$$
$$H(x,y)e^{i(-\omega t+\beta z)}$$

where ω is the angular frequency and β is the propagation constant. The modal effective index is then defined as

$$n_{eff} = \frac{c\beta}{\omega}$$

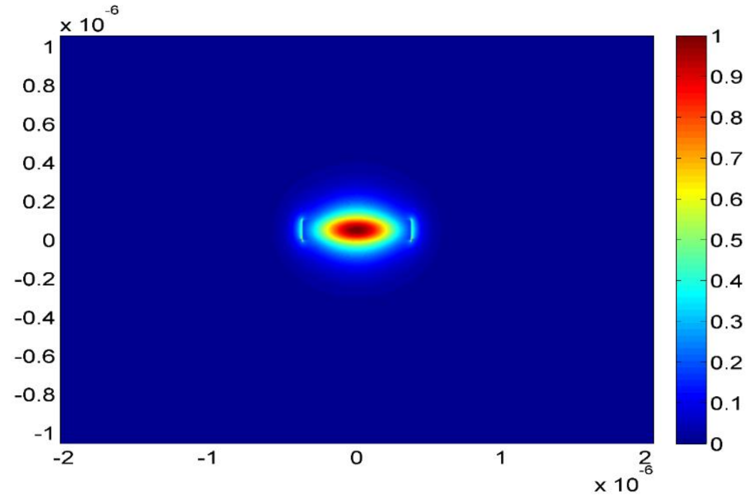

Fig. 4: The intensity distribution of the fundamental mode in silicon waveguide [13]

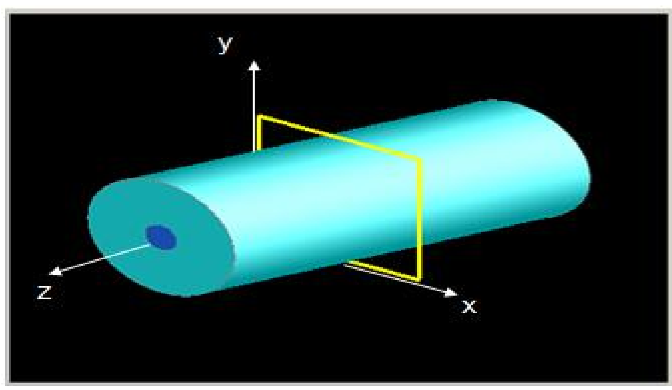

Fig. 5: z-normal eigenmode solver simulation example [1]

The finite-difference algorithm is the current method used for meshing the waveguide geometry and has the ability to accommodate arbitrary waveguide structure. Once the structure is meshed, Maxwell's equations are then formulated into a matrix eigenvalue problem and solved using sparse matrix techniques to obtain the effective index and mode profiles of the waveguide modes.

So, the overall simulation workflow is:

1. Parameters are defined, including the waveguide geometry, doping parameters, contacts, and simulation regions.
2. Electrical simulations are performed to calculate the distribution of electrons and holes in response to the applied voltage. The spatial charge density (2D profile) is exported for each voltage. This simulation will be achieved by the charge transport solver of Lumerical DEVICE.
3. Additional electrical simulations are performed to calculate the device capacitance versus voltage. This simulation will be achieved also by the charge transport solver of Lumerical DEVICE.
4. The charge densities for each voltage from electrical simulation are imported into optical simulator. The plasma dispersion effect is calculated for each corresponding charge density using Soref equations [33]. Optical mode calculations for each voltage are carried out, and the effective refractive index versus voltage is determined. This includes the real and imaginary part of the refractive index.

6. Anticipated Results and Evaluation Criteria

There are two directions in our proposed work.

6.1 Design of integrated optical devices

In our previous work, we introduced new designs of electro-optic modulators with competitive performance [13]–[17]. This device is to be integrated with other photonics components such as ring resonators (RRs) multimode interferometers (MMIs), polarization converters (PCs) and beam steerers. The ultimate objective is to build tunable circuits that serve in optical communications.

Therefore, the criteria to evaluate the performance of our proposed devices will include the set of parameters of the electro-optic modulator besides the specific parameters of each additional component utilizing this modulator. Hence, the evaluation criteria are given in three groups as follows:

6.1.1 The performance parameters of the electro-optic modulator

It is always desirable to use as small voltage for the tuning as possible. As the voltage becomes smaller, the power consumption of the system drops and requirements on the voltage source become less stringent. However, with a smaller voltage, the required modulator size increases [13]–[17]. This means more electrical and optical losses, and hence undesirably high insertion loss and low extinction ratio. This means a compromise is needed and therefore the specific application is what dictates the requirements on voltage and losses. Also, a larger modulator means more electrical capacitance and hence a lower modulation bandwidth.

A good summary of different speed requirements in a network is given in [2] as follows: 1 Pbps for the core transport, 1 Tbps for the metro transport, 100 Gbps for the backhaul truck and finally 1-10 Gbps for the end user devices.

Therefore, in our previous work [13]–[17], we showed different design that can satisfy different applications. Wherever the most important parameter is the speed of modulation (high bandwidth), high voltage can be tolerated. This is the case in the backbone stations where high voltage can be supplied. On the other hand, at the end user device, which might be running on a portable battery, the required voltage must be low $(1-2\,Volt)$ which goes hand-in-hand with relatively lower speed requirements. For example, in our publication [GAA] we introduced the following flavors of the modulators:

Design	$p\ (cm^{-3})$	$z_o\ (nm)$	$V_\pi L_\pi$ $(Volt.cm)$	V $(Volt)$	L (cm)	IL (dB)	$C'(\frac{fF}{\mu m})$	f (GHz)	ER (dB)
I	1×10^{17}	500	5.5	36	0.153	1.8	0.0515	40	28
II	2×10^{17}	300	4.07	40	0.05	4.6	0.053	120	3
III	1×10^{16}	500	5.64	2	0.75	4.9	0.0518	8	3

Here, p is the doping concentration, z_o is the distance between the metallic electrode and the waveguide core and $V_\pi L_\pi$ is the product of the half-wave voltage (V_π) by the corresponding modulator length (L_π). Also, V and L are the tuning voltage and modulator for different operation modes (full or partial modulation), IL is the insertion loss given by the ratio of the optical output power in the high state to the input power, C' is the capacitance per unit length of the modulator, f is the bandwidth and ER is the extension ratio defined as the ratio of the output power high level (on state) to the output low level (off state).

So, based on our experience, we believe there is still room for improvement on these parameters. This improvement can be achieved through more work on optimizing the doping profile of the core of the waveguide and/or adding CMOS compatible tunable materials (such as specific polymer types [25], [26].

6.1.2 The performance parameters of the additional components

As mentioned above, the electro-optic modulator can be more optimized and then integrated with other components to build tunable circuits. Such circuits can be used for routing and power distribution. The performance parameters for each of the candidate components are summarized as follows:

A) Ring resonators (RRs):

A ring resonator offers the feature of having a feedback mechanism in the circuit. Therefore, the RRs can be used as filters, routers and modulators with very high quality factors [42]. Another great feature offered by RRs is the small size of the component which enables high fabrication density. Therefore, the important parameters here are the losses and the size. The loss mechanisms include the waveguide wall scattering losses and the bending losses. The trade-off here is between the ring radius and the bending losses since a smaller ring suffers more losses. With silicon on silica (SOI), the radius can go down to a few micrometers with still acceptable bending losses. As for the scattering losses, this is usually set by the current technology and can be as low as $1\ dB/cm$.

B) Multimode Interferometers (MMIs):

The idea behind this device is allowing the propagation of multiple modes and therefore having the total power profile changing along the propagation direction. This means that the device length determines the lateral power profile at the exit of the device. With simple design rules, this device has been very attractive as a power splitter [36]. Being a multimode device means that the device is inherently large in cross section and hence it is less sensitive to scattering losses and fabrication tolerance. Adding the tuning mechanism to this device means that the power split ratio can be controlled which makes the device act as a router of optical signal. Therefore, the main parameters of performance are the device length, the power split ratio and the extinction ratio.

C) Polarization converters (PCs):

A polarization converter is a component that changes the set of polarization of the optical signal. Typically, in single mode three-dimensional waveguides, polarization converters switch polarization between the transverse electric (TE) like polarization and the transverse magnetic (TM) like mode. In the TE-like mode, the main electric field is parallel to the substrate while in the TM-like mode, the electric field is normal to the substrate. Passive PCs can receive one of the two polarizations and convert it to the other. However, with the tuning mechanism integrated into the PC, the PC can operate as a polarization modulator. This modulator is different from the amplitude modulator in the fact that the two output state, on and off, are given by two different polarizations instead of two different power levels. The main parameters of performance here will be the insertion loss, the extinction ratio and the bandwidth.

D) Beam Steerers:

Beam steerers are used to steer laser in free space. Therefore, beam steerers attracted a lot of attention recently as a solution to wireless optical communications. Besides, they are useful in gas and biomedical detection. A typical beam steering device requires a tuning mechanism which manipulates the phase of a propagating mode and hence the direction of propagation. The performance is measured by the speed of operation, the device size and the accuracy of steering.

6.1.3 The performance parameters of the overall system

In general, the system is required to be efficient on power consumption and on fabrication area. The components should be compatible so that back reflection effects are minimal. This should be achieved through careful layout design of the waveguide dimensions.

6.2 Investigation of the optical characteristics of materials

In our recent work [23], [24], we fabricated and optically characterized doped polymers. The objective is to obtain new materials for optical applications. The material should optimally show low losses in the range of wavelength of interest, which could be the well-known near infrared range ($1.3\ \mu m$ or $1.55\ \mu m$) or the mid infrared range ($\sim 3\ \mu m$). The characterization is conducted using spectrometers in the UV-Vis-NIR range and the MIR range. In this process, the reflection and the transmission of optical power are measured and using reverse engineering, the optical constants of the material are retrieved. Also, the energy gap of the material can be calculated. Manipulating the fabrication parameters, such as temperature and doping, reflect on the material characteristics. So, the measure here is the transmissivity and reflectivity of the material under different fabrication circumstances.

7. Expected Project Outcomes and Impact to AASTMT

I- Technical output and Impact:

a. Design an electro-optic modulator in the mid-infrared range with stronger plasma dispersion effect and less scattering losses.
b. Design a Multimode Interferometers (MMIs) used as a tunable beam splitter at high speeds.
c. TSPC gives inspiration about possible Ph.D thesis.

II- Financial feasibility & Socio-economic Impact:

a. Explore new optical materials which can play a role in the fabrication of integrated optical circuits in the future.

III – Publication:

a. Publish at least a research paper in a Q1-Q2 journal or its equivalent.

8. Resources

Resources are divided into the following parts:

I. Laboratory space: we will need about two types of labs.
   a. Electronics Lab.: normal electronics lab. Equipped by Source meter, one function generator, personal computer and printer. This lab is normally available in AASTMT Cairo campuses. However, spin coater and spray pyrolysis are not available in AASTMT campuses. Spin coater is engineered to provide a high level of rotation accuracy allow for the uniform application of polyimides, metal-organics, dopants, most organic solutions. Spray pyrolysis is required to have additional coating capacity.
   b. Physics Lab.: normal physics lab. Equipped by spectrometer which is available in AASTMT Cairo campuses.
   c. simulation package from Lumerical: With this package, the electronics part of the modulator is simulated using DEVICE where optical simulations are performed to show the optical power modulation.

II. Major equipment:
   1. Source meter
   2. Spin coater
   3. Spray pyrolysis
   4. Spectrometer
   5. Lumerical simulation package

III. Personnel:
   1. Electronics technician: to carry out the technical work.

9. Team Information

Eng. Hany Mahrous:

Eng. Mahrous holds a Master of Science in Electronics and Communications Engineering at the faculty of Engineering and Technology - Arab Academy for Science Technology &Maritime Transport (AASTMT). Eng. Hany,worked on the topic of electro-optic modulators using silicon-on-silica platform. He produced four peer-reviewed journal articles and one conference article [13]–[17] .Eng. Mahrous obtained his B.Sc. degree in Electronics and Electrical Communications Engineering at Menofia University in Egypt. Eng. Mahrous working now as senior lab supervisor and Lab teaching assistant at the Universities of Canada in Egypt.

Assoc. Prof. Michael Gad:

Dr. Gad possesses a strong background in the field of integrated optics [6], [11]–[17], [23]–[25]. Dr. Gad obtained his M. Sc. and Ph.D. degrees from Ain Shams University and University of Waterloo, respectively, in this field where he contributed many publications to the literature. Also, Dr. Gad has done a one year of post-doctor fellowship at University of British Columbia (UBC) in Canada working with an elite team in this field. The publications include theoretical designs [13]–[17] as well as experimental [50], [49],[53], [54],[52],[53]. In his theoretical work, Dr. Gad proposed different active and passive structures using monolithic SOI and hybrid platforms. In his experimental work, Dr. Gad went through two complete cycles of SOI fabrication using IMEC technology in 2009 (Canada) and 2016 (Egypt). He contributed to the design of the layout of the integrated optical circuits and the characterization [49], [53], [54]. Recently, Dr. Gad took interest in the fabrication and characterization of polymer materials for optical applications [23], [24].

Assoc. Prof. Mostafa Fedawy:

Dr. Mostafa Fedawy finished his BSc and Msc. at the Electronics and Communications Department, college of Engineering, Arab Academy for Science and Technology and Maritime Transport, Egypt, at 2001, 2006, respectively. Dr. Fedawy finished his Ph.D. at Ain Shams University, Egypt, 2013 in the field of Devices and nanotechnology. He is currently an Associate Professor at Electronics and Communications Department, College of Engineering, Arab Academy for Science and Technology and Maritime Transport, Egypt.

His research interests include, photovoltaic devices, optoelectronics devices, sensors, simulation and modeling of nanoscale devices including Graphene transistors, TFETs and CNTFETs.

Research Team Information Table

Name of Res. Team Member in English	Name of Res. Team Member in Arabic	University / Institute In English	Position / Title	% of time spent on project	No. of months	Incentive per month (LE)	Number of other projects and their IDs	Total % of time spent on other projects	Contact No
Mostafa Hassan Fedawy	مصطفى حسن فداوي	AASTMT(PI)	Assoc. Prof.	30%	6	2000	-	-	01093738861
Michael Monir Mosaad Gad	ميكل منير مسعد جاد	Ain Shams University	Associate professor	30%	6	2000	-	-	01205399443
Hany Mahrous	هاني محروس	UCE	Eng.	40%	6	2000	-	-	01033337489

10. Project Management

Top Management committee of this project consists of general manager and two teams coordinator. Also, according to teams needs advisors and consultants will join this committee. Management, financial, solving some of technical problems, project orientation and cooperation of all project team members are the main objectives of this committee.

The first team be responsible for multimode interferometers (MMIs) and the second be responsible for investigating new optical materials. Each of the two teams will share their information to maintain all project members with project target. Also team's coordinators will maintain the same objective and cooperation of team members.

The monitoring of the project activities will be delivered through a status and progress reports. A status report should be delivered each month, just to clear the status of the different activities. Its generation is synchronized with the monthly meeting of project group (to be discussed within the meeting). It should be composed of a maximum of one page containing: the red flags, the status of each activity (ongoing/on hold, terminated, etc…). A more detailed technical report should be delivered each 3 months during the project progress. In this progress report, the activity status is described in details with emphasis on the problems and the time monitoring. Finally, a complete report will be delivered at the end of the project.

On the other side, the quality control of the activity achievement could be evaluated using an activity planning sheet and a self-evaluation sheet. The 1st, Activity Planning Sheet (APS) should clearly define, the required goal, the responsible team, the required resources, the time line, the intermediate decision points, and the expected expenses and should be filled at the beginning of any activity. The APS should state deliverables and their timing.

Each one of such sheets enables to control the quality of the jobs achieved. In addition to these sheets, questionnaires will be used in monthly meetings, to obtain the necessary feedback from the working teams. The outputs of the activities related to this part will thus be:

1. Evaluation Sheets.
2. Progress reports.
3. Project final report.

11. Allowable Project Costs

11.1 Major equipment list

Items	Quantity	Estimated cost (LE)
Lumerical simulation package	1	93000 LE
Spin coater	1	85000 LE
Spray pyrolysis	1	33000 LE
Total		210000LE

11.2 Eligible costs

Eligible costs	Break downs		AASTMT support (L.E.)
(A) Staff Cost	Assoc. Prof. Mostafa Fedawy- PI		12000
	Name of each Team member Assoc. Prof. Michael Gad -**Team Coordinator** Eng. Hany Habeeb - **Team Coordinator**		 12000 12000
	Technicians and/or Labor		5000
	Consultation fees		0
	Total		41,000
(B) Equipment	Equipment		210,000
	Spare parts		0
	Total Equipment		210,000
(C) Expendable Supplies & Materials	Stationary		0
	Miscellaneous Laboratory, Field supplies, Materials		15000
	Total expendable Supplies & Materials		15,000
(D) Travel	Internal Transportation		0
	Accommodation		0
	Total travel		0
(E) Other Direct Costs	Services	Manufacture of specimens & prototypes	0
		Acquiring access to specialized reference sources databases or computer software	0
		Computer services	0
	Report preparation		2,000
	Publications & patent Costs		8,500
	Workshops organization or Training		0
	Others[1]		3500
	Total other direct costs		14,000
(G) Total Costs			**280,000**

[1] Internal Transportation

12. Plans for Disseminating Research Results

The results produced are to be reviewed monthly by the principal investigator to be evaluated. Initial promising results will be put in the form of a conference article. The main outcome is expected to be be published in a peer reviewed journal.

The approach of publishing the work will be similar to our recent publications. We do not expect any data to be kept confidential.

12.1 Project Plan

12.1.1 Tasks and activity codes

Code	Main Tasks
T1	Preparation
T2	Design
T3	Simulation
T4	Implementation
T5	Characterization
T6	Publication
T7	Documentation

Code	Activity
A01	Survey
A02	Design
A03	Simulation
A04	Purchase the equipment
A05	Synthesize the new material
A06	Material characterization
A07	Publication
A08	Documentation

12.1.2 A Detailed plan on project's activities (GANTT CHART)

Activity Name	M1	M2	M3	M4	M5	M6	M7	M8	M9	M10	M11	M12
1. Preparation												
1.1 Survey	A01	A01	A01									
2. Design												
2.1 Design			A02	A02	A02							
3. Simulation												
3.1 Simulation			A03	A03	A03	A03						
4 Implementation												
4.1 Purchase the equipment	A04	A04	A04									
4.2 Synthesize the new material				A05	A05	A05	A05					
5. Characterization												
5.1 Material characterization						A06	A06					
6. publication												
6.1 publication							A07	A07	A07	A07		
7. Documentation												
7.1 Documentation											A08	A08

13. References

[1] Lumerical, "High-Performance Nanophotonic Simulation Software - Lumerical," 2019. https://www.lumerical.com/.

[2] S. E. Alavi, M. R. K. Soltanian, I. S. Amiri, M. Khalily, A. S. M. Supa'at, and H. Ahmad, "Towards 5G: A Photonic Based Millimeter Wave Signal Generation for Applying in 5G Access Fronthaul," Sci. Rep., vol. 6, pp. 1–11, 2016.

[3] C. Gunn, "CMOS photonics for high-speed interconnects," IEEE Micro, vol. 26, no. 2, pp. 58–66, 2006.

[4] E. Jaberansary, "New Computational Method to Estimate The Effect of Roughness On Scattering Loss and Its Implementation In a Hybrid Heterojunction Optical Modulator," University of Southampton, 2004.

[5] "Chromosol's silicon photonics system tackles data transfer bottleneck | Business | Chemistry World." https://www.chemistryworld.com/news/chromosols-silicon-photonics-system-tackles-data-transfer-bottleneck/4013135.article (accessed Mar. 02, 2021).

[6] M. Gad, A. Zaki, and Y. M. Sabry, "Silicon photonic mid-infrared grating coupler based on silicon-on-insulator technology," Natl. Radio Sci. Conf. NRSC, Proc., pp. 400–406, 2017.

[7] R. Halir et al., "An ultra-compact multimode interference coupler with a subwavelength grating slot," Laser Photonics Rev., vol. 7, no. 2, 2013.

[8] C. A. Barrios, "Integrated microring resonator sensor arrays for labs-on-chips," Anal. Bioanal. Chem., vol. 403, no. 6, pp. 1467–1475, 2012.

[9] V. Van Member, T. A. Ibrahim, P. P. Absil, F. G. Johnson, R. Grover, and P. T. Ho, "Optical signal processing using nonlinear semiconductor microring resonators," IEEE J. Sel. Top. Quantum Electron., vol. 8, no. 3, pp. 705–713, 2002.

[10] C. Brooks, "Passive silicon-on-insulator polarization-rotating waveguides," Opt. Eng., vol. 45, no. 4, p. 44603, 2006.

[11] M. Gad, D. Yevick, and P. Jessop, "Compound ring resonator circuit for integrated optics applications," J. Opt. Soc. Am. A, vol. 26, no. 9, p. 2023, 2009.

[12] M. Gad, D. Yevick, and P. Jessop, "High sensitivity ring resonator gyroscopes," Fiber Integr. Opt., vol. 30, no. 6, pp. 395–410, 2011.

[13] H. Mahrous, M. Gad, M. El Sabbagh, M. Fedawy, and W. Fikry, "A High-Speed Electro-Optic Modulator with Optimized Electrode Positions," Proc. - 2018 13th Int. Conf. Comput. Eng. Syst. ICCES 2018, vol. 2, no. 1, pp. 530–535, 2019.

[14] H. Mahrous, M. Fedawy, M. El Sabbagh, W. Fikry, and M. Gad, "Design of a 90 GHz SOI fin electro-optic modulator for high-speed applications," Appl. Sci., vol. 9, no. 22, 2019.

[15] H. Mahrous, M. Fedawy, M. El Sabbagh, W. Fikry, and M. Gad, "130 Gbps low-loss electro-optic modulator based on metal-oxide-semiconductor technology," Optik (Stuttg)., vol. 217, 2020.

[16] H. Mahrous, M. Fedawy, M. El Sabbagh, W. Fikry, and M. Gad, "A compact 120 GHz monolithic silicon-on-silica electro-optic modulator," Opt. Quantum Electron., vol. 52, no. 2, 2020.

[17] H. Mahrous et al., "Design of compact, high-speed and low-loss silicon-on-silica electro-optic modulators," Semicond. Sci. Technol., vol. 35, no. 9, Jun. 2020.

[18] J. Wang et al., "Silicon high-speed binary phase-shift keying modulator with a single-drive push–pull high-speed traveling wave electrode," Photonics Res., vol. 3, no. 3, p. 58, 2015.

[19] G. T. Reed, G. Mashanovich, F. Y. Gardes, and D. J. Thomson, "Silicon optical modulators," Nat. Photonics, vol. 4, no. 8, pp. 518–526, 2010.

[20] T. Hiraki et al., "Heterogeneously integrated III-V/Si MOS capacitor Mach-Zehnder modulator," Nat. Photonics, vol. 11, no. 8, pp. 482–485, 2017.

[21] R. A. Soref, S. J. Emelett, and W. R. Buchwald, “Silicon waveguided components for the long-wave infrared region*,” J. Opt. A Pure Appl. Opt, vol. 8, pp. 840–848, 2006.
[22] J. Hodgkinson and R. P. Tatam, “Optical gas sensing: A review,” Meas. Sci. Technol., vol. 24, no. 1, 2013.
[23] M. Salah, M. Gad, M. Elkattan, and Y. Sabry, “Optical constants of gamma-irradiated silver-doped PVA in the near-infrared range,” Micro Nano Lett., vol. 15, no. 7, pp. 480–485, 2020.
[24] M. Salah, M. Gad, M. Elkattan, and Y. M. Sabry, “Effect of gamma-irradiation and doping on the absorption edge and the optical bandgap of silver-doped PVA films,” Opt. Commun., vol. 473, no. October 2019, p. 125933, 2020.
[25] M. Gad, D. Yevick, and P. E. Jessop, “Tunable polymer/silicon over insulator ring resonators,” Opt. Eng., vol. 47, no. 12, p. 124601, Dec. 2008.
[26] G. Yevick, David, Michael, “High-speed polymer/silicon on insulator ring resonator switch,” Opt. Eng., vol. 47, no. 9, p. 094601, 2008.
[27] X. Xiao et al., “High-speed, low-loss silicon Mach–Zehnder modulators with doping optimization,” Opt. Express, vol. 21, no. 4, p. 4116, 2013.
[28] G. T. Reed et al., “Recent breakthroughs in carrier depletion based silicon optical modulators,” Nanophotonics, vol. 3, no. 4–5, pp. 229–245, 2014.
[29] G. Li et al., “Ring resonator modulators in silicon for interchip photonic links,” IEEE J. Sel. Top. Quantum Electron., vol. 19, no. 6, 2013.
[30] C. Wang, M. Zhang, B. Stern, M. Lipson, and M. Lončar, “Nanophotonic lithium niobate electro-optic modulators,” Opt. Express, vol. 26, no. 2, p. 1547, 2018.
[31] P. O. Weigel et al., “Hybrid Silicon Photonic-Lithium Niobate Electro-Optic Mach-Zehnder Modulator Beyond 100 GHz Bandwidth,” pp. 1–19, 2018, [Online]. Available: http://arxiv.org/abs/1803.10365.
[32] N. C. Harris et al., “Efficient, compact and low loss thermo-optic phase shifter in silicon,” Opt. Express, vol. 22, no. 9, p. 10487, 2014.
[33] R. A. Soref and B. R. Bennett, “Electrooptical effects in silicon,” IEEE J. Quantum Electron., vol. 23, no. 1, pp. 123–129, 1987.
[34] R. Marchetti et al., “Low-loss micro-resonator filters fabricated in silicon by CMOS-compatible lithographic techniques: Design and characterization,” Appl. Sci., vol. 7, no. 2, pp. 1–11, 2017.
[35] W. Wang et al., “A CMOS compatible 1x3 optical switch based on silicon on insulator,” IEEE Int. Conf. Gr. IV Photonics GFP, pp. 207–209, 2010.
[36] A. Ortega-Moñux et al., “An ultra-compact multimode interference coupler with a subwavelength grating slot,” Laser Photonics Rev., vol. 7, no. 2, 2013.
[37] W. D. Sacher, T. Barwicz, B. J. F. Taylor, and J. K. S. Poon, “Polarization rotator-splitters in standard active silicon photonics platforms,” Opt. Express, vol. 22, no. 4, p. 3777, 2014.
[38] S. A. Miller et al., “Large-scale optical phased array using a low-power multi-pass silicon photonic platform,” Optica, vol. 7, no. 1, p. 3, 2020.
[39] T. Baehr-Jones et al., “Ultralow drive voltage silicon traveling-wave modulator,” Opt. Express, vol. 20, no. 11, p. 12014, 2012.
[40] L. Chrostowski and M. Hochberg, Silicon photonics design. 2015.
[41] “CHARGE solver introduction – Lumerical Support.” https://support.lumerical.com/hc/en-us/articles/360034917693-CHARGE-solver-introduction (accessed Mar. 08, 2021).
[42] W. Bogaerts et al., “Silicon microring resonators,” Laser and Photonics Reviews, vol. 6, no. 1. pp. 47–73, Jan. 2012.

14. Declaration of original submission and Other Grant(s)

By signing below, I acknowledge that I have read, understand and accept to comply with all the terms of the foregoing application, mentioned in AASTMT general conditions and guidelines for submitting a research proposal, including, but not limited to:

- The total number of the application pages should not exceed 30 pages excluding a cover page, as well as all sections of the proposal (as mentioned in AASTMT General Conditions and Guidelines for Submitting Research Proposal).
- At any time, a contracted AASTMT project team member should only be participating in a maximum of one project.
- Allowable budget maximum limit should be strictly adhered to in the project proposal. In all cases, requested budget has to be justified in detail.
- AASTMT guidelines, IPR rules, code of ethics, etc. (www.aast.edu), should be read carefully and adhered to. These are integral parts of the contract.
- All proposals – in addition to PI and other data - must be uploaded to the AASTMT website by the designated deadline. Uploaded PI data should conform to the corresponding data in the application form.

Applications will not be considered eligible and will be discarded in the following cases:

- Proposals submitted by e-mail or sent as hard copies or uploaded to the AASTMT website after the deadline.
- Proposals not conforming to the designated format.
- Proposals whose uploaded PI data does not conform to PI data in the proposal file.
- Proposals in which the allowable budget maximum limit has been exceeded.
- Proposals in which maximum allowable contracted AASTMT project participation limit has been exceeded.
- Proposal letter does not include a scanned copy of the signed and stamped PI institution endorsement letter in case of team member work outside AASTMT.
- Proposal does not include a scanned copy of the signed acknowledgment form.

Date & Signature: Mostafa Fedawy ______________________________